X Workshop em Engenharia e Tecnologia Espaciais
7 a 9 de agosto de 2019

Reaction Rate of $\mathrm{HCCO}\,(^2\mathrm{A})$ via TST

EUCLIDES, H. O. [1], **BARRETO, P. R. P.** [1]

[1] Instituto Nacional de Pesquisas Espaciais, São José dos Campos, SP, Brasil
Aluno de Doutorado do curso de Ciência e Tecnologia de Materiais e Sensores - CMS.

henriqueuclides@gmail.com

Abstract

In this work, we present the reaction rate and dissociation of ketenyl radical HCCO, where we found two possible pathways for the doublet state $(^2\mathrm{A})$. The optimized geometries and frequencies were determined at B3LYP/6-311g(2d,d,p) internal to CBS-QB3 methods. The reaction rates are calculated using the APUAMA code, applying the tunneling correction of Wigner, Eckart and small curvature transmission coefficient (SCT), and the total reaction rate is presented in the Arrhenius form as $\mathrm{k}_{(^2\mathrm{A})}(\mathrm{s}^{-1}) = 3.16 \times 10^{58}\mathrm{T}^{-57.21}\exp(-361.01\,\mathrm{kcal\,mol}^{-1}/\mathrm{RT})$.

Keywords: Rate constant; Quantum chemistry; HCCO; Ketenyl radical.

1. Introduction

The ketenyl radical, HCCO, is an organic molecule found mainly in interstellar clouds, both in clouds around young stellar objects and in cold dark clouds [Agúndez et al. 2015]. In the first case, ketenyl radical molecules are probably formed on the dust grain surface and released into the gas phase by thermal evaporation [Herbst and van Dishoeck 2009], whereas in dark clouds, the chemical composition is characterized by highly unsaturated carbon chains of the polyyne families (organic compound with alternation between singlet and triplet) and relatively simple organic molecules containing oxygen, whose synthesis depends largely on chemical processes in the gas phase [Agúndez and Wakelam 2013]. Therefore, a better understanding of dark cloud chemistry must necessarily imply deep observational studies capable of increasing both the number of chemically characterized sources and the inventory of molecules identified.

The objective of this work is to present the reaction rate of ketenyl radical by optimizing the geometries (interatomic distances and angles), calculating frequencies of the species and comparing with experimental data to present accuracy of our calculation. For the reaction rate, we have used the APUAMA code [Euclides and Barreto 2017] with the transition state theory (TST) applying tunneling correction of Wigner [Wigner 1932], Eckart [Eckart 1930] and SCT [Gonzalez-Lafont et al. 1991] in a temperature range of $200-4000$K (which is the standard temperature range used in APUAMA).

Section 2 describes our electronic structure calculations, section 3 discuss the results and 4 presents concluding remarks.

2. Methodology

2.1. *Ab initio* calculations

For the *ab initio* calculations we used B3LYP/6-311g(2d,d,p) method internal to CBS-QB3 which computes very accurate energies. For all species used: reactants, products and transition

state structures, the geometries and frequencies was determined and the energy was calculated. The number of imaginary frequencies, 1 or 0, determine if we have a transition state or the reactants and products, respectively. All this calculations were performed using the GAUSSIAN09 program.

2.2. Reaction rate with APUAMA

We use the APUAMA [Euclides and Barreto 2017] code to calculate the thermodynamic properties and reaction rate using TST (transition state theory). The equation of TST is given:

$$k(T) = \frac{k_B T}{h} \frac{Q_{X^\ddagger}}{Q_A Q_{BC}} \exp\left(-\frac{V_a^{G^\ddagger}}{RT}\right) \tag{1}$$

Where the constants are k_B for Boltzmann, h for Planck and R for gas constant, the partition functions $Q_{X^\ddagger}$, Q_A and Q_{BC} are given by the products of partition functions of translation, rotation, vibration and eletronic. The entry for APUAMA [Euclides and Barreto 2017] are all the properly defined species and their data, like the mass, external symmetry, geometry, frequencies, energy and imaginary frequency for transition state. The outputs of the program are: the rate with three types of tunneling: Wigner [Wigner 1932] which uses a parabolic potential for the nuclear motion near the transitions structure, taking into account only the imaginary frequency and not the reaction coordinate; Eckart [Eckart 1930] which is the ratio between the coefficients of quantum and classical reaction; and small curvature transmission coefficient (SCT) [Gonzalez-Lafont et al. 1991] which is approximated by the ratio of the fundamental state probabilities by the classical state. The rate is presented in the Arrhenius form [Arrhenius 1889], the thermodynamic properties such as entropy, enthalpy and heat capacity are calculated and the minimum energy path with ZPE (zero-point energy) correction and the reaction barriers as well.

3. Results and Discussions

Two reaction paths were found for the doublet state, both lead to the same product $\mathrm{CCO} + \mathrm{H}$, defined by:

$$\mathrm{HCCO} \underset{k_{-1}}{\overset{k_1}{\rightleftarrows}} \mathrm{HC_2O} \underset{k_{-2}}{\overset{k_2}{\rightleftarrows}} \mathrm{HC_2O} \underset{k_{-3}}{\overset{k_3}{\rightleftarrows}} \mathrm{HOCC} \underset{k_{-4}}{\overset{k_4}{\rightleftarrows}} \mathrm{HOCC} \overset{k_5}{\rightarrow} \mathrm{CCO} + \mathrm{H} \qquad \text{(PW1)}$$

$$\mathrm{HCCO} \underset{k_{-6}}{\overset{k_6}{\rightleftarrows}} \mathrm{HOCC} \underset{k_{-4}}{\overset{k_4}{\rightleftarrows}} \mathrm{HOCC} \overset{k_5}{\rightarrow} \mathrm{CCO} + \mathrm{H} \qquad \text{(PW2)}$$

The figure 1 presents the PES (potential energy surface) for the two reaction paths of $\mathrm{HCCO}\ (^2\mathrm{A})$. In the first reaction path PW1 we have a barrier of $72.6\,\mathrm{kcalmol^{-1}}$ ($60.9\,\mathrm{kcalmol^{-1}}$ [Zhao et al. 2007] CCSD(T)//B3LYP/6-311G(d,p)) to pass through TS1 and form $\mathrm{HC_2O}$ with an energy of $52.9\,\mathrm{kcalmol^{-1}}$ ($52.7\,\mathrm{kcalmol^{-1}}$ [Zhao et al. 2007]), then we have an exchange reaction of $\mathrm{HC_2O}$ with a barrier of $50.5\,\mathrm{kcalmol^{-1}}$ to cross the TS2, to form HOCC with energy of $55.8\,\mathrm{kcalmol^{-1}}$ ($55.0\,\mathrm{kcalmol^{-1}}$ [Zhao et al. 2007]) we have the TS3 with a barrier of $57.1\,\mathrm{kcalmol^{-1}}$ ($54.9\,\mathrm{kcalmol^{-1}}$ [Zhao et al. 2007]), TS4 is a exchange reaction of HOCC with a barrier of $53.3\,\mathrm{kcalmol^{-1}}$, and to form the product $\mathrm{CCO} + \mathrm{H}$ with energy of $118.04\,\mathrm{kcalmol^{-1}}$ ($92.7\,\mathrm{kcalmol^{-1}}$ [Zhao et al. 2007]) it is necessary to traverse TS5 with a barrier of $65.5\,\mathrm{kcalmol^{-1}}$ ($45.4\,\mathrm{kcalmol^{-1}}$ [Zhao et al. 2007]). In the last reaction path PW2 we have TS6 with a barrier of $99.7\,\mathrm{kcalmol^{-1}}$ to form HOCC from the reagent HCCO.

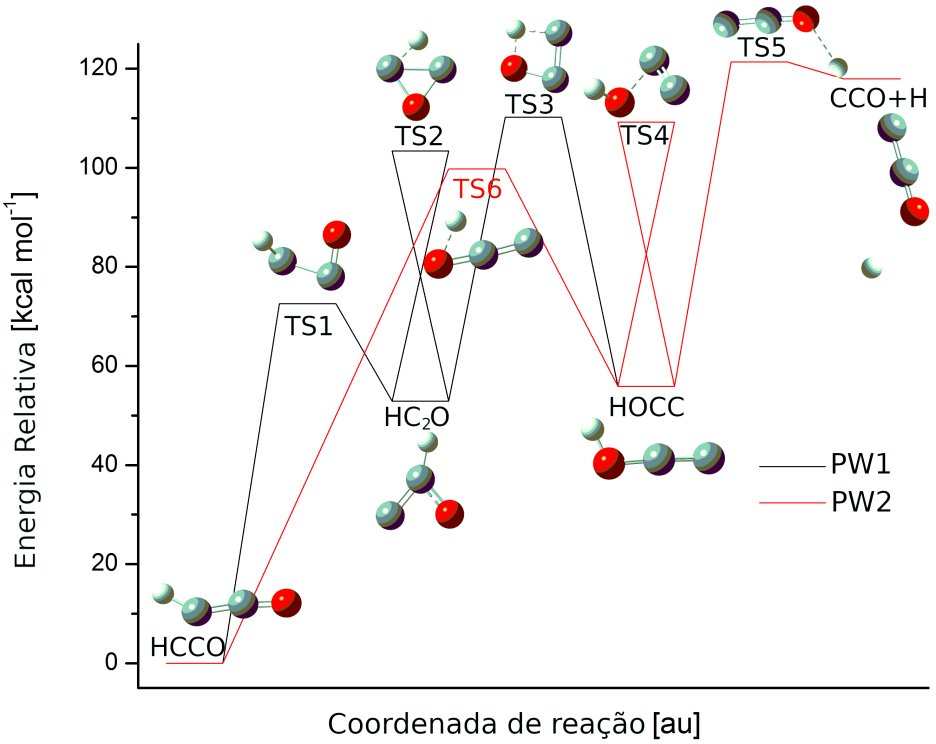

Figura 1. PES for the two pathways of $\mathrm{HCCO}\ (^2\mathrm{A})$

The figure 2 shows all species calculated for the ketenyl radical in the doublet state and when possible were compared with the reference. The table 1 shows the vibrational and ZPE frequencies for all species and TS of the $\mathrm{HCCO}\ (^2\mathrm{A})$. As for the geometries, the vibrational frequencies calculated at 6-311G(2d,d,p) compared to the respective references show less difference in the values when compared with smaller bases. For HCCO, HOCC, and $\mathrm{H_2CO}\ (^2\mathrm{A''})$ the frequencies differ with [Zhao et al. 2007] in (0.6, 0.4, 0.4, 0.4, 0.1, 0.4) $\mathrm{cm^{-1}}$, (13.4, 0.7, 0.4, 0.1, 2.6, 0.4) $\mathrm{cm^{-1}}$ and (0.8, 0.5, 0.8, 2.7, 0.5, 1.3) $\mathrm{cm^{-1}}$, respectively. The frequencies of the $\mathrm{TS3}\ (^2\mathrm{A})$ was compared with [Zhao et al. 2007] differing in (1.4, 0.6, 0.4, 0.1, 0.1, 1.3) $\mathrm{cm^{-1}}$.

The IRC calculation [Schlegel 1989] is shown in the figure 3(a)-(f). The figure 3(a) shows the decrease of the distance $\mathrm{R_{CO}}$ responsible for the change in the almost planar geometry of HCCO to $\mathrm{HC_2O}$ while the distance $\mathrm{R_{C'O}}$ has a small variation of up to $0.4\mathring{A}$; the angles $\mathrm{A_{C'CO}}$ and $\mathrm{A_{HCO}}$ vary from about $45°$ to about $25°$, respectively, while the dihedral angle $\mathrm{A_{HCCO}}$ ranges from 180 up to $68°$ in the transition structure and then back to $180°$. In the figure 3(b) we see a transition structure, where the hydrogen atom exchanges the bond of one carbon with the other, so the distances $\mathrm{R_{HC'}}$ and $\mathrm{R_{HC}}$ also vary in opposite directions; the dihedral angle $\mathrm{A_{HCCO}}$ varies up to the transition structure and returns to the same point, while the angle $\mathrm{A_{HCC'}}$ varies up to $125°$. The figure 3(c) shows the formation of the bond HO by decreasing the distance $\mathrm{R_{HO}}$, and the distance of the atoms CO with decreasing the distance $\mathrm{R_{CO}}$ due to the increase of the angle $\mathrm{A_{CC'O}}$, the angle $\mathrm{A_{HCO}}$ varies around $100°$. Fig. 3(d) shows a further exchange reaction such as the figure 3(b), where the oxygen changes carbon and we observe this in the variations of the distances $\mathrm{R_{CO}}$ and $\mathrm{R_{C'O}}$ increasing and decreasing respectively; the dihedral angle $\mathrm{A_{HCCO}}$ has a slight variation around the transition structure and the angle $\mathrm{A_{C'CO}}$ decreases by up to $70°$. In the figure 3(e) we have the product formation $\mathrm{CCO + H}$, where the distance $\mathrm{R_{HO}}$ increases by breaking the bond HO and the angle $\mathrm{A_{OCC'}}$ varies slightly to make the molecule OCC' planar, the distances $\mathrm{R_{CO}}$ and $\mathrm{R_{CC'}}$ are kept almost constant. The figure 3(f) shows the hydrogen atom

exchanging the carbon bond for oxygen, this is observed by the variations in the distances R_{HO} and $R_{HC'}$ decreases and increases respectively; the angle $A_{CC'H}$ varies from about 30° while A_{COH} varies up to 70°.

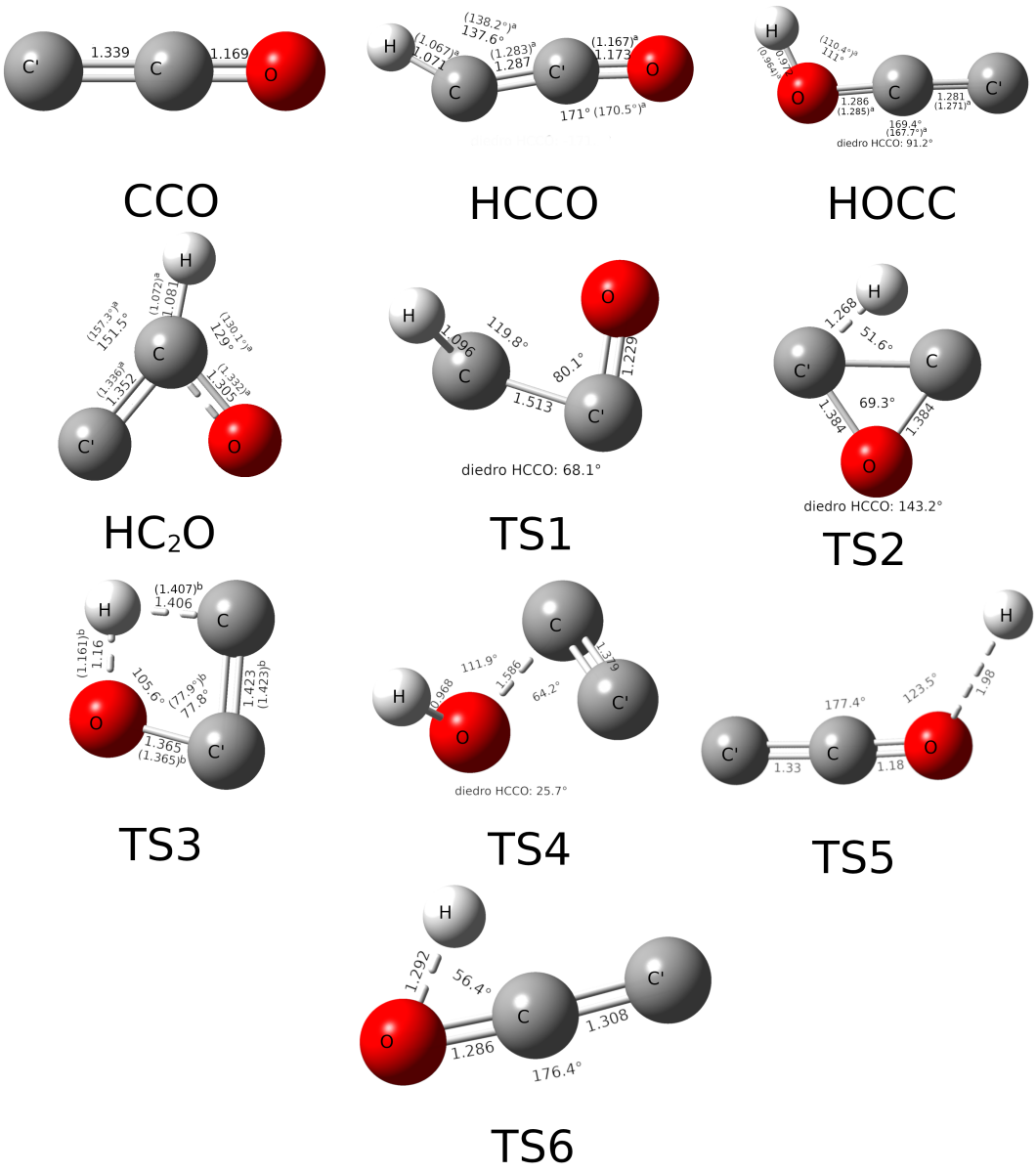

Figura 2. Optimized geometries for calculated species in B3LYP/6-311G(2d,d,p) of $HCCO\ (^2A)$**. Å for distances and degree for angles**

[a][Sattelmeyer et al. 2004] e [b][Zhao et al. 2007]

Tabela 1. Vibrational frequencies (cm^{-1}) and ZPE ($kcal\ mol^{-1}$) for all species and TS of HCCO (^{2}A)

Specie		6-31G(d)	6-311G(d)	6-311G(2d,d,p)	ref
CCO (^{1}A)	ν_i	447.9, 1118.5, 2043.7	307.4, 1113.2, 2044.4	307.4, 1113.2, 2044.4	
	EPZ	5.16	4.95	4.95	
HCCO (^{2}A)	ν_i	492.2, 513.6, 542.1	494.3, 508.2, 566.1	440.4, 508.6, 564.4	441, 509, 564[b]
		1268.8, 2097.2, 3368.4	1263.8, 2091.4, 3342.3	1269.6, 2092.1, 3354.6	1270, 2092, 3355
	EPZ	11.84	11.81	11.76	
HOCC (^{2}A)	ν_i	215.3, 321.5, 1076.0	199.3, 329.7, 1070.4	206.4, 332.7, 1070.4	193, 332, 1070[b]
		1263.7, 1974.1, 3589.8	1274.0, 1982.5, 3627.4	1257.1, 1979.4, 3668.6	1257, 1982, 3669
	EPZ	12.06	12.12	12.17	
HC_2O (^{2}A″)	ν_i	324.0, 803.9, 1043.5	299.0, 816.5, 1038.2	303.2, 824.5, 1039.8	304, 823, 1039[b]
		1311.5, 1559.3, 3254.3	1307.2, 1549.1, 3216.6	1299.7, 1551.5, 3218.7	1297, 1552, 3220
	EPZ	11.86	11.76	11.77	
$TS1$ (^2A)	ν_i	775.6*i*, 518.6, 670.4	742.1*i*, 465.0, 660.8	755.1*i*, 459.4, 655.9	
		1032.1, 1565.8, 3102.9	1031.2, 1579.2, 3088.9	1017.1, 1577.4, 3079.5	
	EPZ	9.84	9.75	9.70	
$TS2$ (^2A)	ν_i	1008.1*i*, 603.2, 783.8	987.9*i*, 599.1, 794.0	950.3*i*, 583.1, 796.3	
		1033.2, 1286.1, 2229.4	1030.9, 1289.7, 2245.5	1011.8, 1289.4, 2262.7	
	EPZ	8.48	8.51	8.49	
$TS3$ (^2A)	ν_i	1237.3*i*, 634.0, 828.0	1352.8*i*, 620.9, 836.3	1312.6*i*, 618.4, 821.6	1314*i*, 619, 822[b]
		1104.1, 1293.6, 2103.1	1083.9, 1291.6, 2045.1	1086.9, 1297.9, 2124.3	1087, 1298, 2123
	EPZ	8.52	8.40	8.50	
$TS4$ (^2A)	ν_i	341.0*i*, 580.9, 739.8	315.9*i*, 607.1, 741.7	320.2*i*, 601.3, 710.6	
		1065.5, 1307.9, 3674.7	1040.9, 1319.9, 3716.3	1002.7, 1318.8, 3745.5	
	EPZ	10.53	10.61	10.54	
$TS5$ (^2A)	ν_i	444.1*i*, 234.9, 407.1	499.7*i*, 248.0, 426.7	482.2*i*, 240.9, 420.4	
		500.6, 1133.0, 1944.4	530.1, 1130.5, 1931.3	529.1, 1129.3, 1936.8	
	EPZ	6.03	6.09	6.08	
$TS6$ (^2A)	ν_i	1893.7*i*, 235.6, 349.8		1902.2*i*, 262.8, 341.2	
		1059.1, 1816.2, 2534.5		1059.9, 1822.4, 2540.9	
	EPZ	8.57		8.61	

[b][Zhao et al. 2007]

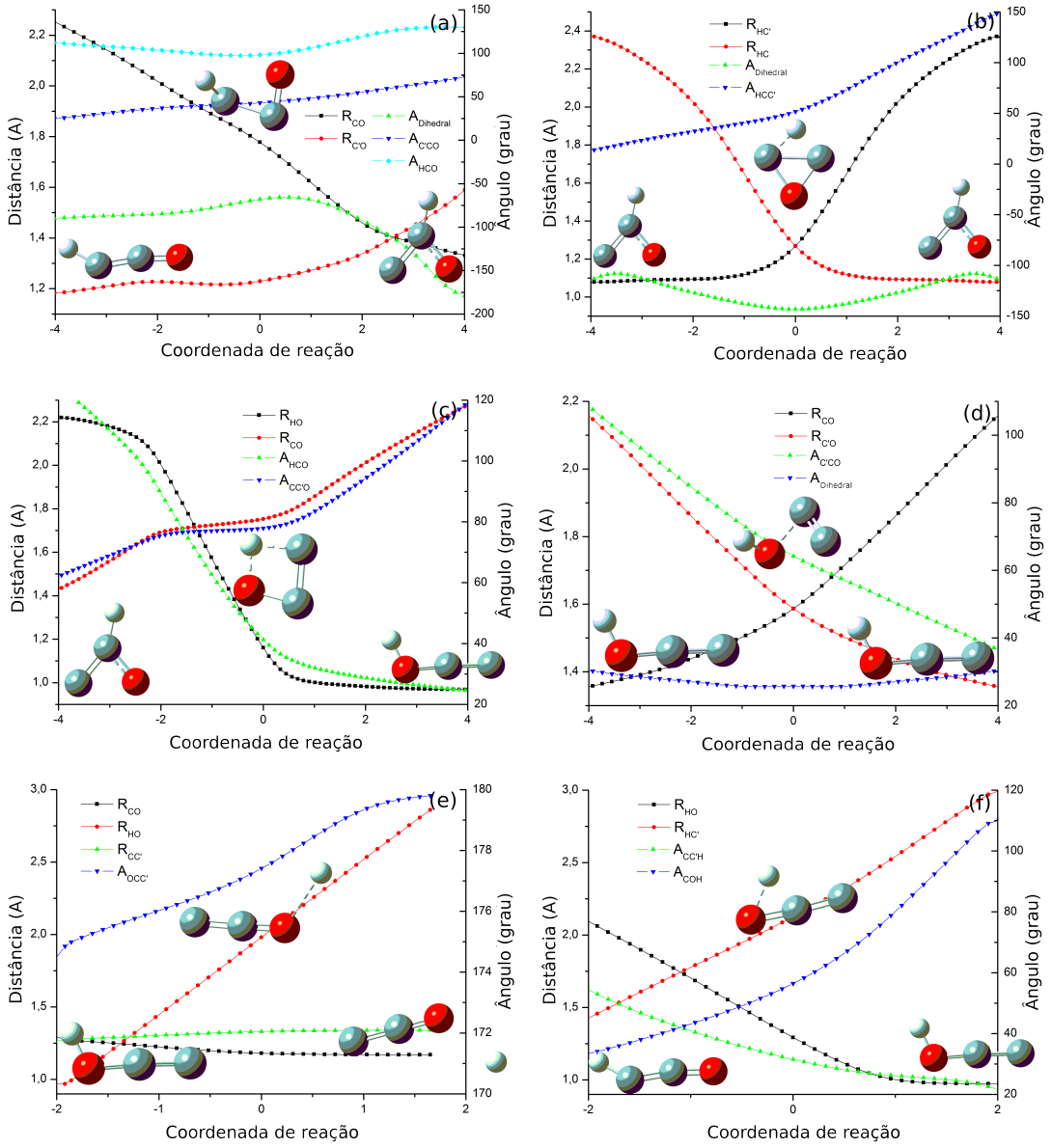

Figura 3. The bond lengths and bond angle changes along the reaction coordinate of $HCCO\,(^2A)$ **for (a) TS1, (b) TS2, (c) TS3, (d) TS4, (e) TS5 and (f) TS6**

3.1. Reaction rate

For the first reaction path PW1, we apply the steady-state condition, and the reaction rate is given by the equation:

$$k_{PW1} = \frac{k_1 k_3 k_5}{k_3 k_{-3} - (k_{-3} + k_4 - k_{-4} + k_5)(k_2 - k_{-2} + k_3 + k_{-1})} \tag{2}$$

The reaction rate for the second pathway PW2, is defined by:

$$k_{PW2} = \frac{k_5 k_6}{k_4 - k_{-4} + k_5 + k_{-6}} \tag{3}$$

The global rate for the doublet system is given:

$$k_{tot} = k_5 \left(\frac{k_6}{k_4 - k_{-4} + k_5 + k_{-6}} + \frac{k_1 k_3}{k_3 k_{-3} - (k_{-3} + k_4 - k_{-4} + k_5)(k_2 - k_{-2} + k_3 + k_{-1})} \right) \tag{4}$$

The reaction rate for the $\mathrm{HCCO}\,(^2\mathrm{A})$ is shown in figure 4(a), where we compare the rates for each reaction path PW1 and PW2 together with the overall rate using SCT tunneling. The branching rate was calculated to determine which reaction paths are most likely to occur. In the figure 4(b), we show the branching rates for the doublet state in a temperature range of 200-4000K, we can observe that the reaction path PW2 is more likely to occur with a probability of almost 63% at high temperatures, while the PW1 path has 37% occurring at temperatures close to 4000K.

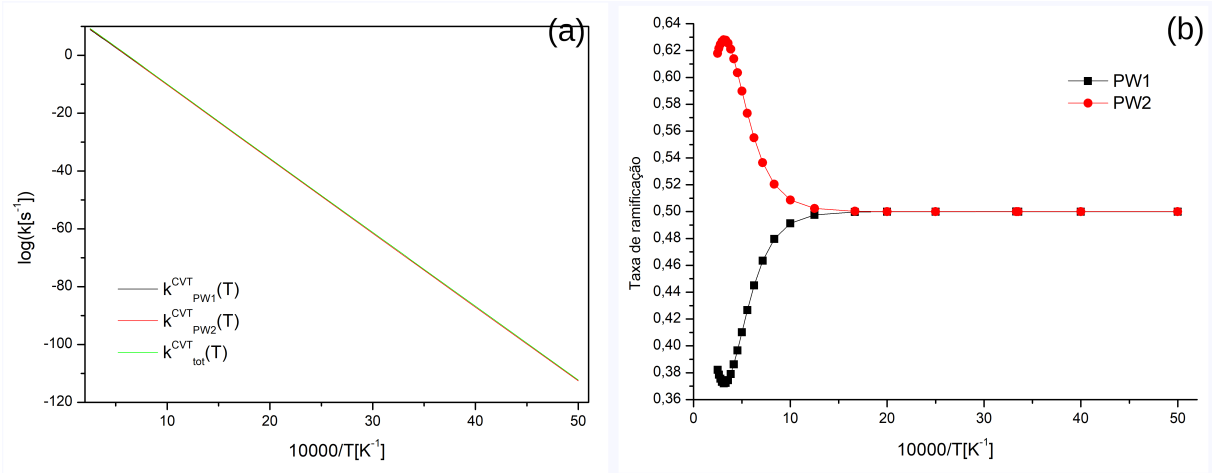

Figura 4. Reaction rate with SCT (a) and branching rates (b) for both reaction pathways of $\mathrm{HCCO}\,(^2\mathrm{A})$

4. Conclusion

In this paper, we have used the transition state and electronic structure theory to describe possible dissociation pathways for ketenyl radical in doublet state. The geometries of the species that compose the PES were calculated with B3LYP in 6-311G(2d,d,p) basis set, where we can confirm the pathways using IRC calculation, and the energy was calculated at CBS-QB3 for higher accuracy. The reaction rate was calculated in a temperature range of 200-4000K with APUAMA code. The branching ratio calculated confirms that PW2 is more probable to occurs. The total reaction rate can be represented in Arrhenius form with SCT as:

$$\mathrm{k}_{(^2\mathrm{A})}(\mathrm{s}^{-1}) = 3.16 \times 10^{58} \mathrm{T}^{-57.21} \exp(-361.01\,\mathrm{kcal\,mol}^{-1}/\mathrm{RT})$$

Comparing our calculations with experimental data we can confirm good aggrement for the geometry parameters, vibrational frequencies and reaction rates.

Acknowledgements: *This work has been supported by CAPES.*

Referências

Agúndez, M., Cernicharo, J., and Guélin, M. (2015). Discovery of interstellar ketenyl (hcco), a surprisingly abundant radical. *Astronomy and Astrophysics*, 50, n.5:577.

Agúndez, M. and Wakelam, V. (2013). Chemistry of dark clouds: Databases, networks, and models. *Chemical Reviews*, 113:8710.

Arrhenius, S. A. (1889). On the reaction rate of the inversion of non-refined sugar upon souring. *Zeitschrift fr Physikalische Chemie*, 4:226.

Eckart, C. (1930). The penetration of a potential barrier by electrons. *The Physical Review*, 35:1303–1309.

Euclides, H. O. and Barreto, P. R. P. (2017). Apuama: a software tool for reaction rate calculations. *Journal of Molecular Modelling*, 23:176.

Gonzalez-Lafont, A., Truong, T. N., and Truhlar, D. G. (1991). Interpolated variational transition-state theory: Practical methods for estimating variational transition-state properties and tunneling contributions to chemical reaction rates from electronic structure calculations. *Journal of Chemical Physics*, 95:8875.

Herbst, E. and van Dishoeck, E. F. (2009). Complex organic interstellar molecules. *Annual Review of Astronomy & Astrophysics*, 47:427.

Sattelmeyer, K. W., Yamaguchi, Y., and III, H. F. S. (2004). Energetics of the low-lying isomers of hcco. *Chemical Physics Letters*, 383:266–269.

Schlegel, C. G. H. B. (1989). An improved algorithm for reaction path following. *Journal of Chemical Physics*, 90:2154–2161.

Wigner, E. (1932). ber die geschwindigkeitskonstanten von austauschreaktionen. *Zeitschrift fr Physikalische Chemie*, 15:445.

Zhao, X., Zhang, J., Liu, J., Li, X., and Li, Z. (2007). Theoretical study on the mechanism of the $\mathrm{c_2h} + \mathrm{o}$ reaction. *Chemical Physics Letters*, 436:41–46.